Electronic Supplementary Material (ESI) for ChemComm.
This journal is © The Royal Society of Chemistry 2019

Electronic Supplementary Information for

Host-guest Interaction Enabled Chiroptical Photo-switching and Enhanced Circularly Polarized Luminescence

Lukang Ji,[a,b] Qianwen He,[c] Dian Niu,[a,b] Jiajing Tan,[c] Guanghui Ouyang*[a] and Minghua Liu*[a,b]

E-mail: ouyanggh@iccas.ac.cn, liumh@iccas.ac.cn.

[a] Beijing National Laboratory for Molecular Science (BNLMS), CAS Key Laboratory of Colloid, Interface and Chemical Thermodynamics, Institute of Chemistry, Chinese Academy of Sciences, Beijing, 100190, China.

[b] University of Chinese Academy of Sciences, Beijing, 100490, China.

[c] Beijing University of Chemical Technology, Beijing, 100029, China.

Contents

1. Supplementary Data for NMR Job's plot experiments, ITC and rheology data.

2. SEM and TEM images of CG hydrogel and CG⊂CyD supra-hydrogels.

3. SEM and TEM images of CG and CG⊂CyD hydrogels after UV irradiation.

4. Supplementary spectra for CG and CG⊂CyD hydrogels before and after UV irradiation.

5. Supplementary NMR data for CG and CG⊂CyD.

6. Supplementary XRD, FT-IR and DLS data.

7. Experimental Section.

1. Supplementary Data for NMR Job's plot experiments.

(a)

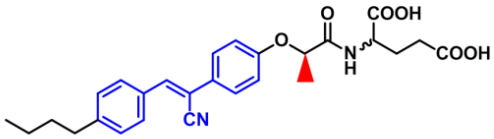

Entry	Host	Guest	X=[G]/([G]+[H])	δ	Δδ	Δδ*X
1	0 eq	1.0 eq	1	4.2659	0	0
2	0.1 eq	0.9 eq	0.9	4.3039	0.038	0.0342
3	0.2 eq	0.8 eq	0.8	4.3617	0.0958	0.07664
4	0.3 eq	0.7 eq	0.7	4.4138	0.1479	0.10353
5	0.4 eq	0.6 eq	0.6	4.4856	0.2197	0.13182
6	0.5 eq	0.5 eq	0.5	4.5284	0.2625	0.13125
7	0.6 eq	0.4 eq	0.4	4.5688	0.3029	0.12116
8	0.7 eq	0.3 eq	0.3	4.5979	0.332	0.0996
9	0.8 eq	0.2 eq	0.2	4.6133	0.3474	0.06948
10	0.9 eq	0.1 eq	0.1	4.6301	0.3642	0.03642
11	1.0 eq	0 eq	0			0

(b)

Entry	Host	Guest	X=[G]/([G]+[H])	δ	Δδ	Δδ*X
1	0 eq	1.0 eq	1.0	4.2659	0	0
2	0.1 eq	0.9 eq	0.9	4.3030	0.0371	0.03339
3	0.2 eq	0.8 eq	0.8	4.3516	0.0857	0.06856
4	0.3 eq	0.7 eq	0.7	4.4179	0.152	0.1064
5	0.4 eq	0.6 eq	0.6	4.5095	0.2436	0.14616
6	0.5 eq	0.5 eq	0.5	4.5552	0.2893	0.14465
7	0.6 eq	0.4 eq	0.4	4.6015	0.3356	0.13424
8	0.7 eq	0.3 eq	0.3	4.6399	0.374	0.1122
9	0.8 eq	0.2 eq	0.2	4.6419	0.376	0.0752
10	0.9 eq	0.1 eq	0.1	4.6448	0.3789	0.03789
11	1.0 eq	0 eq	0			0

(c)

Entry	Host	Guest	X=[G]/([G]+[H])	δ	Δδ	Δδ*[G]
1	0 eq	1.0 eq	1	4.1702	0	
2	0.1 eq	0.9 eq	0.9	4.1919	0.0217	0.01953
3	0.2 eq	0.8 eq	0.8	4.2529	0.0827	0.06616
4	0.3 eq	0.7 eq	0.7	4.3072	0.137	0.0959
5	0.4 eq	0.6 eq	0.6	4.3462	0.176	0.1056
6	0.5 eq	0.5 eq	0.5	4.4193	0.2491	0.12455
7	0.6 eq	0.4 eq	0.4	4.4654	0.2952	0.11808
8	0.7 eq	0.3 eq	0.3	4.4602	0.29	0.087
9	0.8 eq	0.2 eq	0.2	4.4576	0.2874	0.05748
10	0.9 eq	0.1 eq	0.1	4.5340	0.3638	0.03638
11	1.0 eq	0 eq	0			

Table S1. NMR data used for Job plot analyses. The protons of the alkoxyl was selected for the Job's plot analyses. Host is CyD, guest is CG. [CyD] + [CG] = 4.3 mM: (a) CG⊂α-CyD. (b) CG⊂β-CyD. (c) CG⊂γ-CyD. Notes: due to the poor solubility of CG in water, its lithium salt was used, which was named as CG-Li.

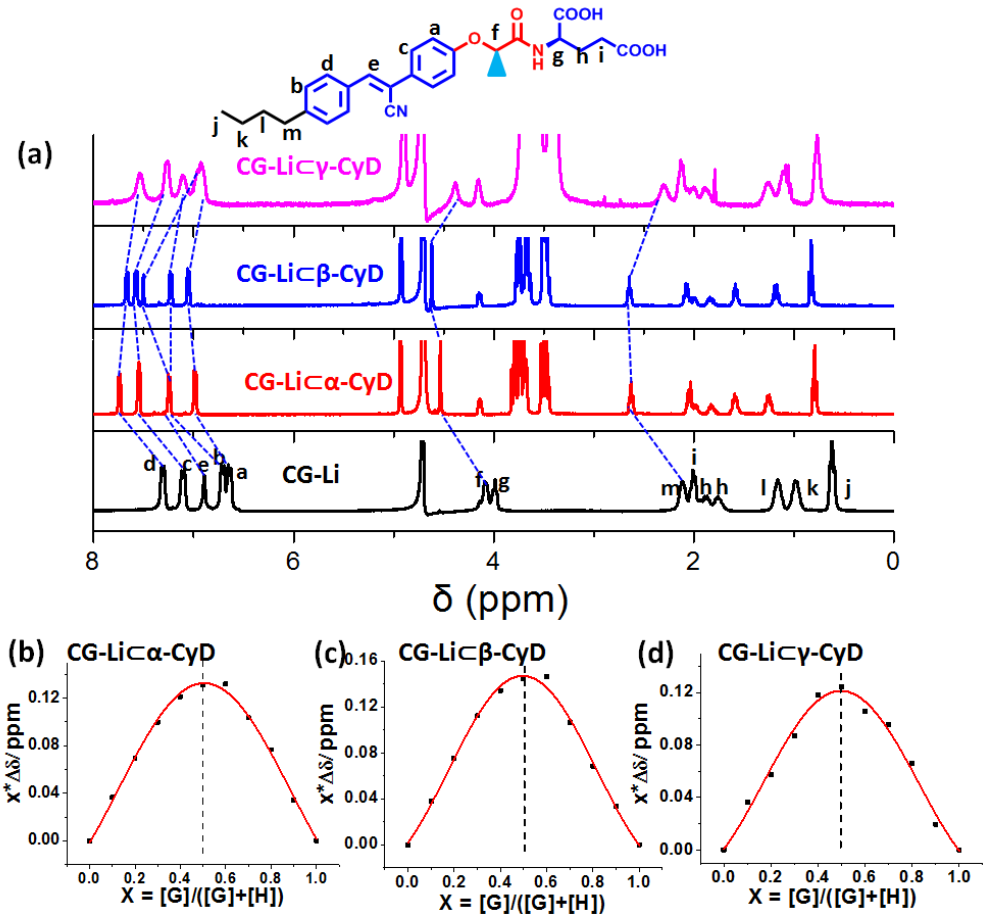

Figure S1. ^{1}H NMR titration experiments. (a) Stacked ^{1}H NMR partial spectra for CG-Li and CG-Li⊂CyDs (400 MHz, D_2O, 298K, [CG-Li] = 2.15 mM, [CyD] = 2.15 mM). (b)-(d) Job's plot for the CG-Li/CyDs complex (D_2O, 298K, [CyD] + [CG-Li] = 4.3 mM).

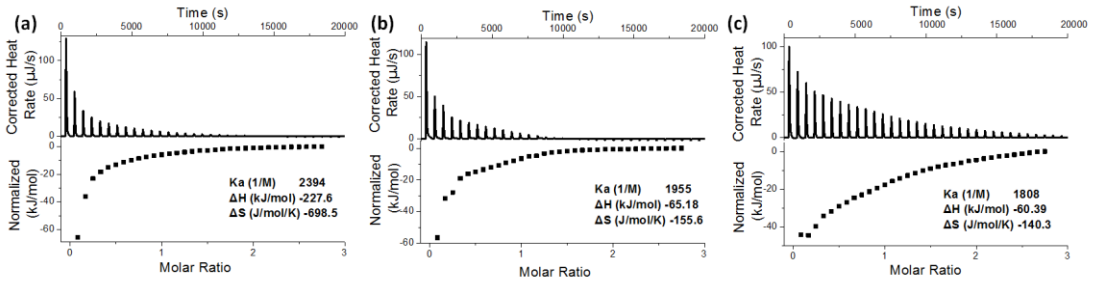

Host	Guest	K (M^{-1})
α-CyD	CG-Li	$2.39x10^3$
β-CyD	CG-Li	$1.96x10^3$
γ-CyD	CG-Li	$1.81x10^3$

Figure S2. ITC (Isothermal Titration Calorimetry) titration curve of (a) α, (b) β or (c) γ-CyD with CG-Li in pure water at 298 K. Raw ITC data for 33 sequential injections (10.0 μL per injection) of a CG-Li solution (10.0 mM) into CyDs solution (2.0 mM).

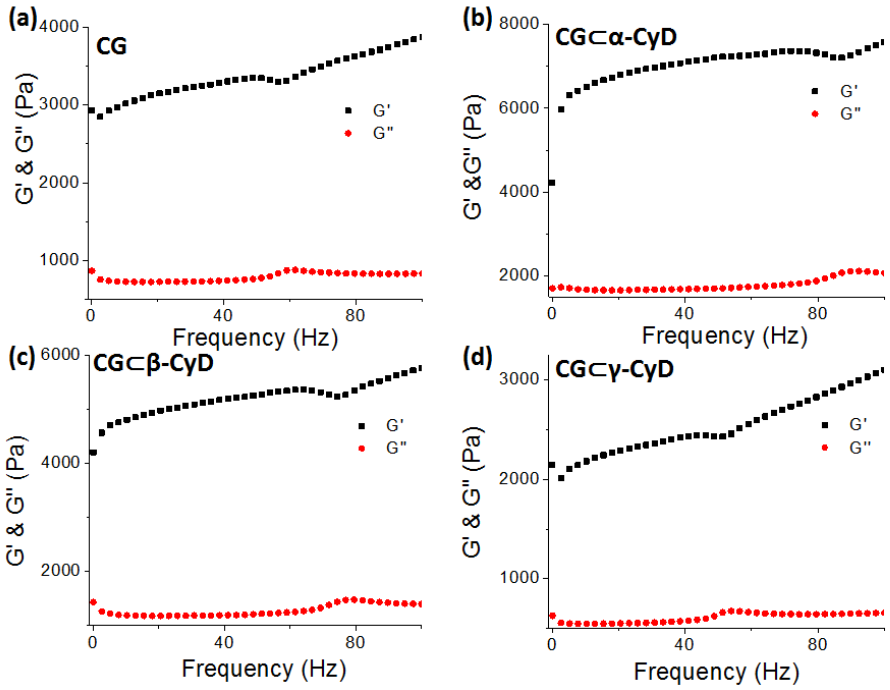

Figure S3. Rheological studies of hydrogels: (a) CG hydrogel, (b) CG⊂α-CyD supra-hydrogel, (c) CG⊂β-CyD supra-hydrogel, (d) CG⊂γ-CyD supra-hydrogel. [CG] = [CyDs] = 6.5 mM.

The storage modulus (G') is 3-4 times larger than the loss modulus (G'') in all the three supra-hydrogels, which indicated that they are elastic rather than viscous material. Such rheological result is a characteristic of gel materials. However, the mechanical strength of CG⊂α-CyD supra-hydrogel and CG⊂β-CyD supra-hydrogel was increased while the CG⊂γ-CyD supra-hydrogel was decreased compared with that of CG hydrogel, which might be one reason for different photo-reversibility for the three supra-gelator.

2. SEM and TEM images of CG hydrogel and CG⊂CyD supra-hydrogels.

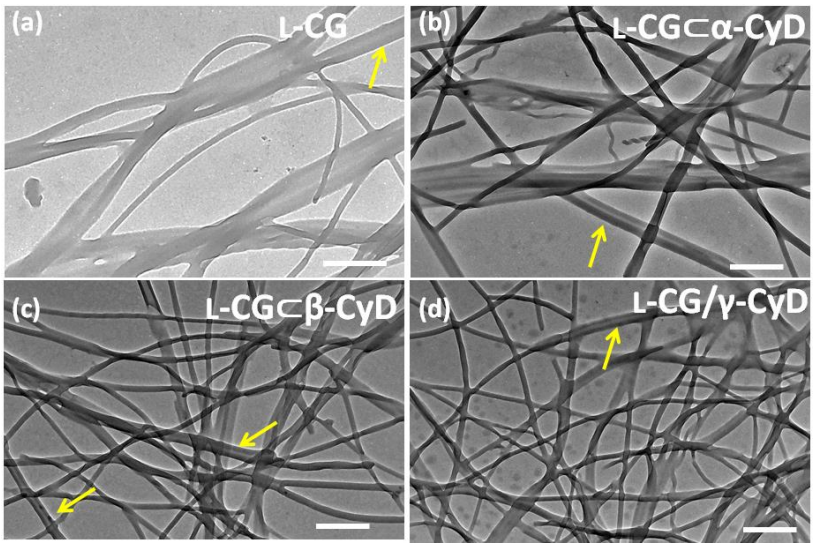

Figure S4. TEM images of the hydrogel of (a) L-CG, (b) L-CG⊂α-CyD, (c) L-CG⊂β-CyD (d) L-CG⊂γ-CyD. Scale bar 500 nm. [CG] = [CyD] = 6.5 mM. Nanotube structures could be clearly observed for all the four samples.

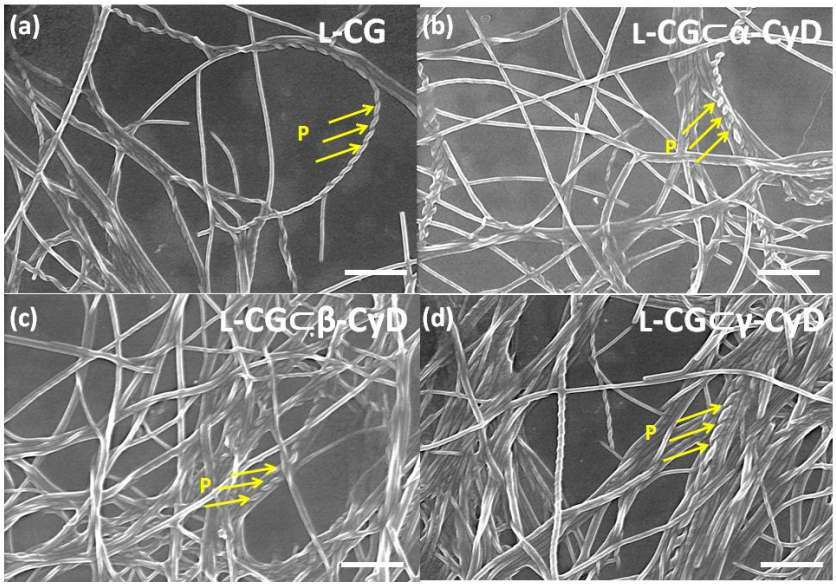

Figure S5. SEM images showed right-handed nanotubes and nanohelices for the hydrogels of (a) L-CG, (b) L-CG⊂α-CyD, (c) L-CG⊂β-CyD (d) L-CG⊂γ-CyD. Scale bar 500 nm. [CG] = [CyD] = 6.5 mM.

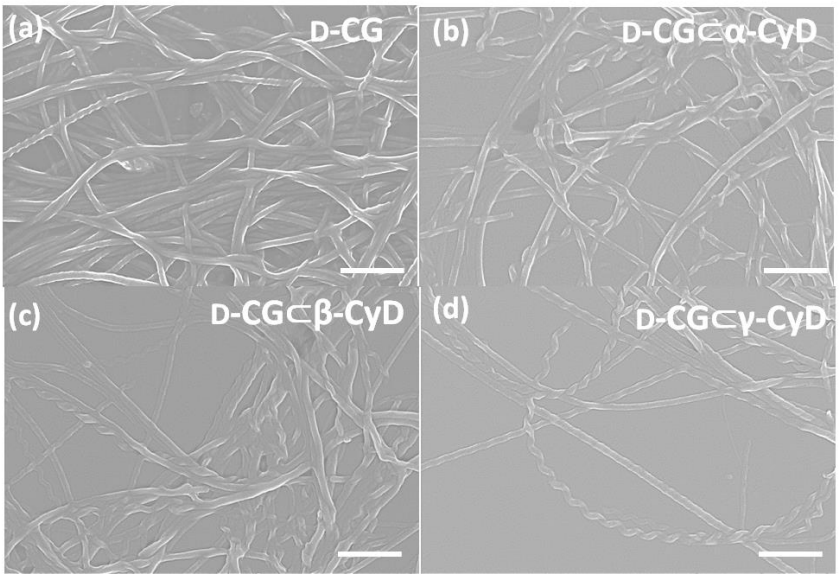

Figure S6. SEM images showed left-handed nanotubes and nanohelices for the hydrogels of (a) D-CG, (b) D-CG⊂α-CyD, (c) D-CG⊂β-CyD (d) D-CG⊂γ-CyD. Scale bar 500 nm. [CG] = [CyD] = 6.5 mM.

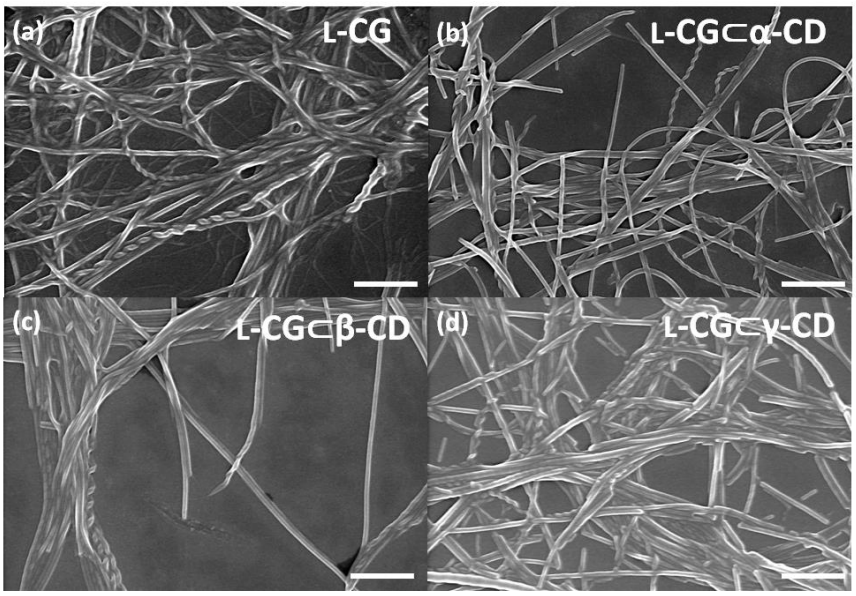

Figure S7. SEM images of high concentration hydrogels, [CG] = [CyD] = 13 mM. (a) L-CG, (b) L-CG⊂α-CyD, (c) L-CG⊂β-CyD (d) L-CG⊂γ-CyD. Scale bar 500 nm.

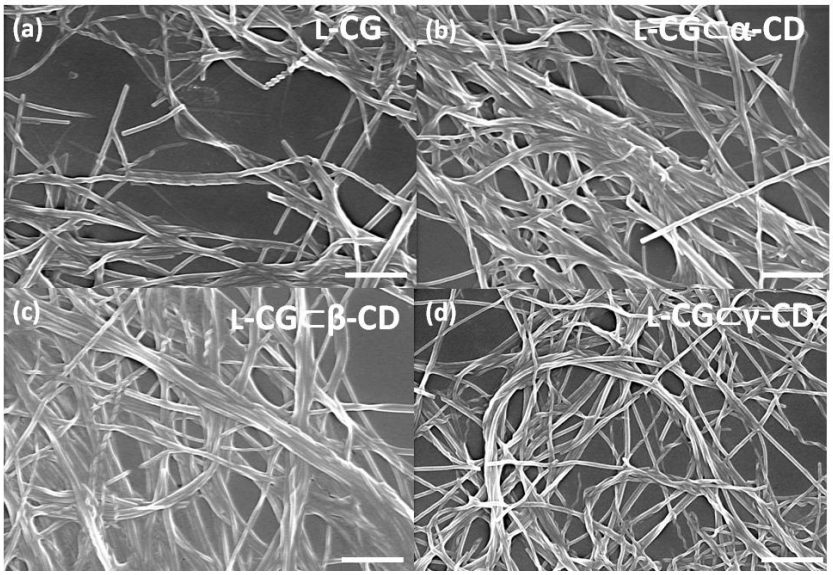

Figure S8. SEM images of high concentration hydrogels, [CG] = [CyD] = 19.5 mM. (a) L-CG, (b) L-CG⊂α-CyD, (c) L-CG⊂β-CyD (d) L-CG⊂γ-CyD. Scale bar 500 nm.

3. SEM images of CG and CG⊂CyD hydrogels after UV irradiation.

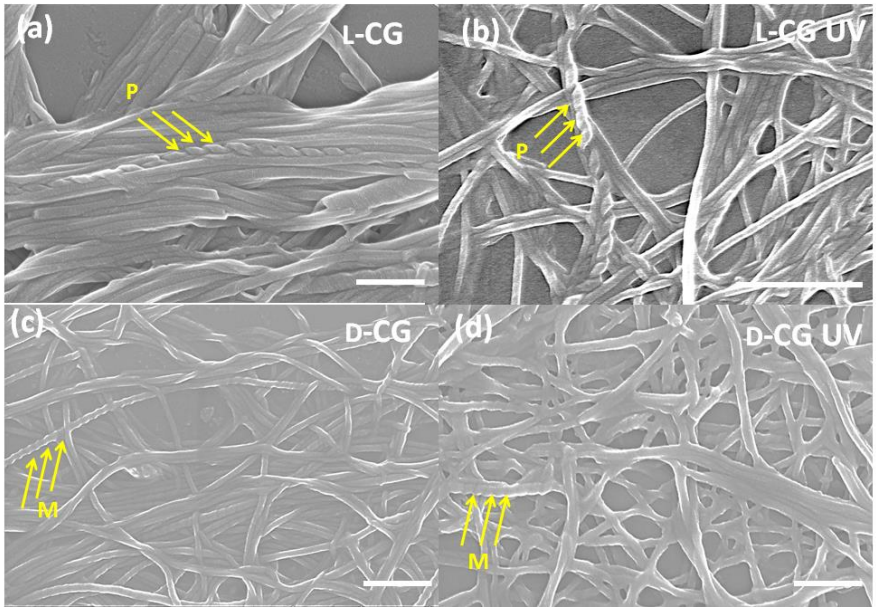

Figure S9. SEM images demonstrated that the nanostructures of L- and D-CG hydrogels are remained after 2 hours UV irradiation. (a) L-CG hydrogel, (b) L-CG hydrogel after UV irradiation, (c) D-CG hydrogel, (d) D-CG hydrogel after UV irradiation. Scale bar 500 nm. [CG] = 6.5 mM.

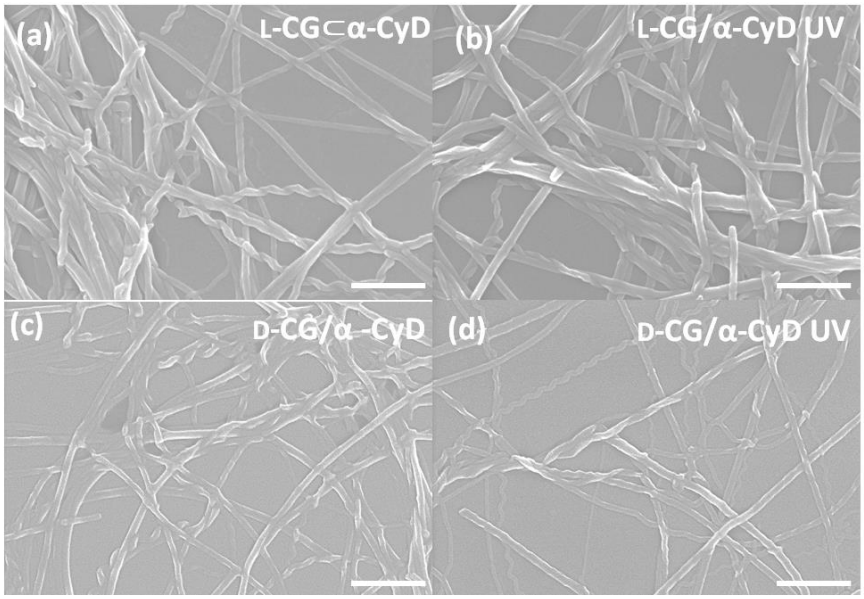

Figure S10. SEM images demonstrated that the nanostructures of L- and D-CG⊂α-CyD supra-hydrogels are remained after 2 hours UV irradiation. (a) L-CG⊂α-CyD hydrogel, (b) L-CG⊂α-CyD hydrogel after UV irradiation, (c) D-CG⊂α-CyD hydrogel, (d) D-CG⊂α-CyD hydrogel after UV irradiation. Scale bar 500 nm. [CG] = [CyD] = 6.5 mM.

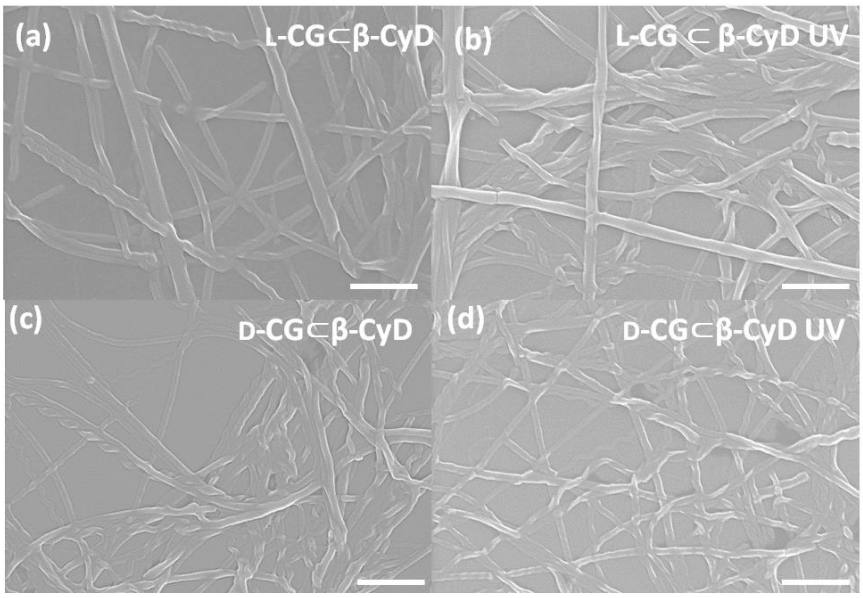

Figure S11. SEM images demonstrated that the nanostructures of L- and D-CG⊂β-CyD supra-hydrogels are remained after 2 hours UV irradiation. (a) L-CG⊂β-CyD hydrogel, (b) L-CG⊂β-CyD hydrogel after UV irradiation, (c) D-CG⊂β-CyD hydrogel, (d) D-CG⊂β-CyD hydrogel after UV irradiation. Scale bar 500 nm. [CG] = [CyD] = 6.5 mM.

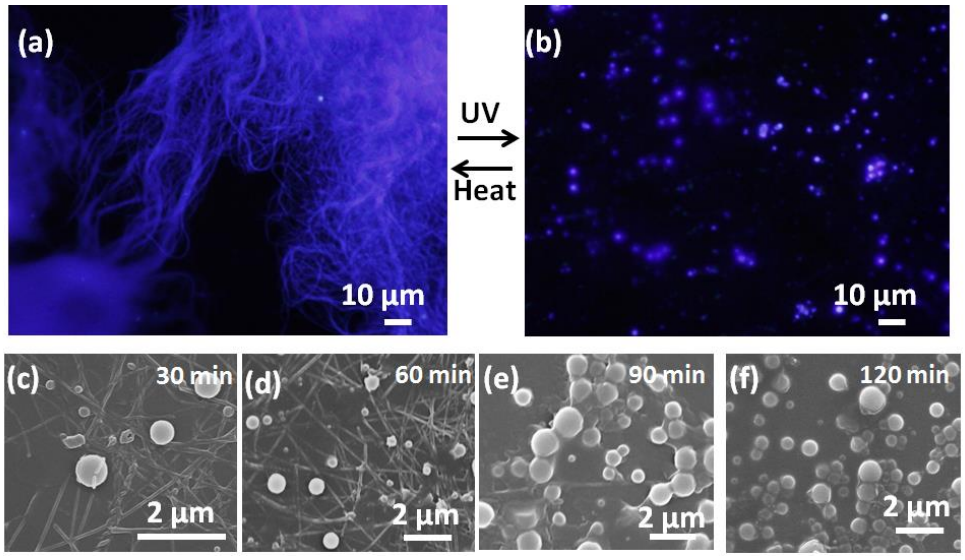

Figure S12. Fluorescence microscope images of the (a) nanotubes and (b) the nanospheres. Morphological evolution (c)-(f) of CG⊂γ-CyD nanostructures with different UV irradiation time.

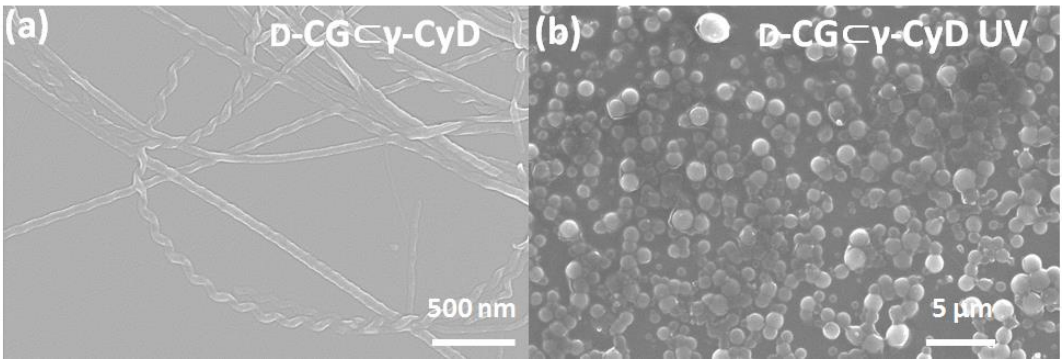

Figure S13. SEM images of (a) D-CG⊂γ-CyD supra-hydrogel and (b) D-CG⊂γ-CyD supra-hydrogel after 2 hours UV irradiation. [CG] = [γ-CyD] = 6.5 mM.

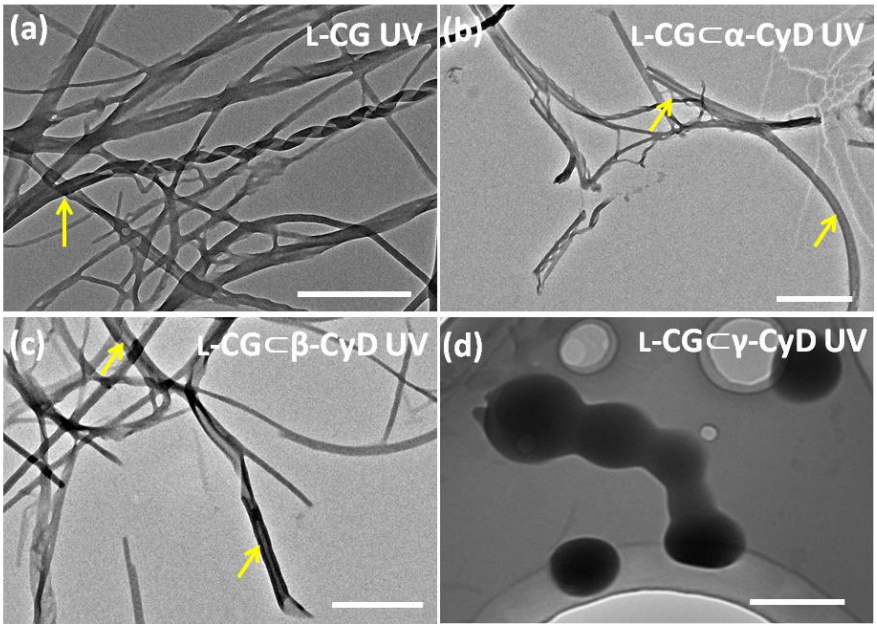

Figure S14. TEM images of (a) L-CG hydrogel after UV, (b) L-CG⊂α-CyD supra-hydrogel after UV, (c) L-CG⊂β-CyD supra-hydrogel after UV, (d) L-CG⊂γ-CyD supra-hydrogel after UV. [CG] = [CyD] = 6.5 mM. Scale bar 1 μm.

4. Supplementary spectra for CG and CG⊂CyD hydrogels before and after UV irradiation.

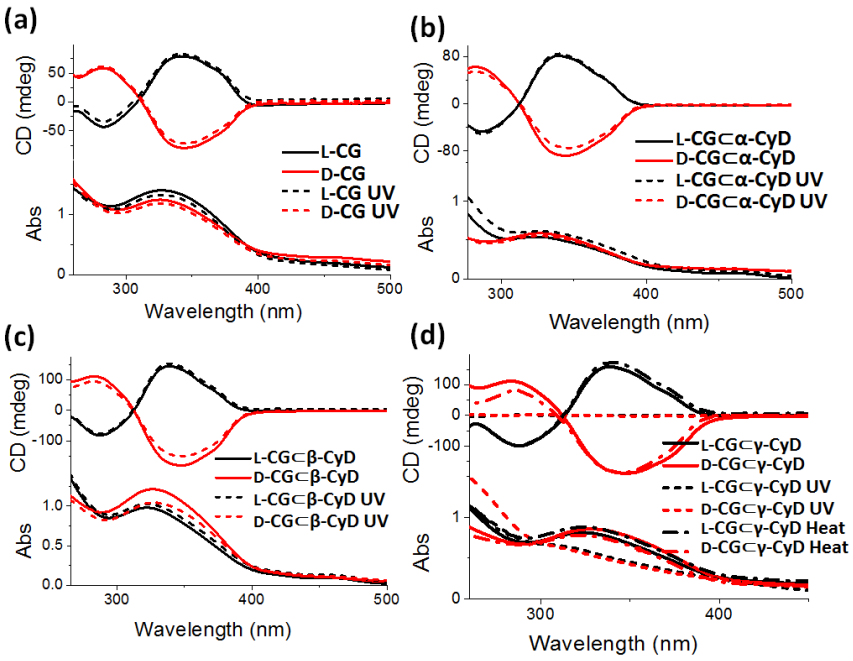

Figure S15. CD spectra of CG and CG⊂CyD hydrogels before and after UV irradiation. (a) CG, (b) CG⊂α-CyD, (c) CG⊂β-CyD, (d) CG⊂γ-CyD. Notes: the black lines are corresponding to L-CG related hydrogels, while the red lines are D-CG related hydrogels. [CG] = [CyD] = 6.5 mM.

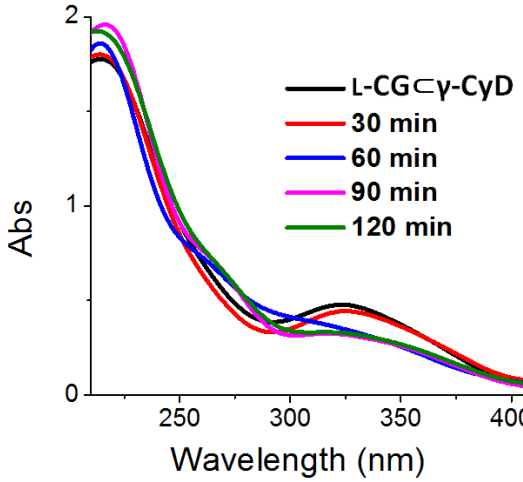

Figure S16. UV-Vis spectra of CG⊂γ-CyD hydrogel under different UV irradiation times. [CG] = [γ-CyD] = 6.5 mM.

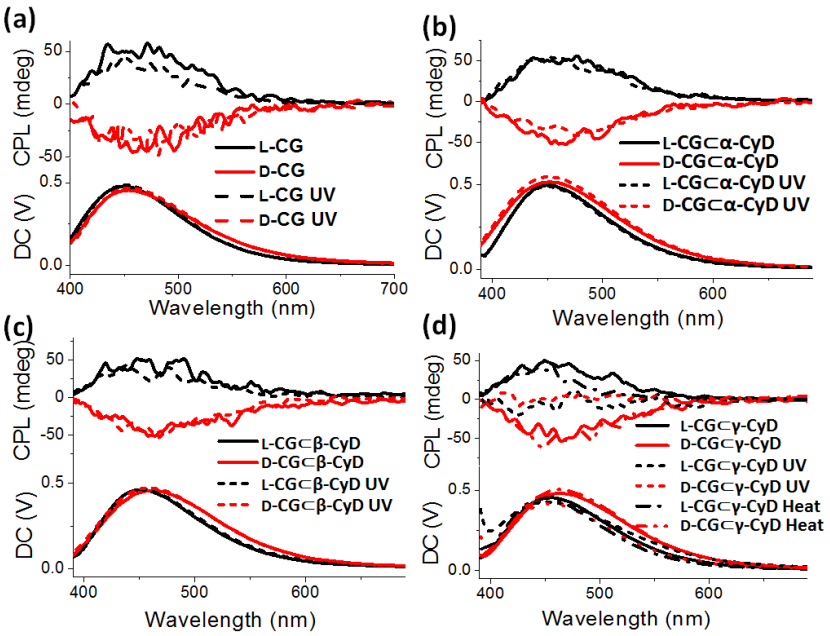

Figure S17. CPL spectra of CG and CG⊂CyD hydrogels before and after UV irradiation. (a) CG, (b) CG⊂α-CyD, (c) CG⊂β-CyD, (d) CG⊂γ-CyD. Notes: the black lines are corresponding to L-CG related hydrogels, while the red lines are D-CG related hydrogels. [CG] = [CyD] = 6.5 mM.

5. Supplementary NMR data for CG and CG⊂CyDs.

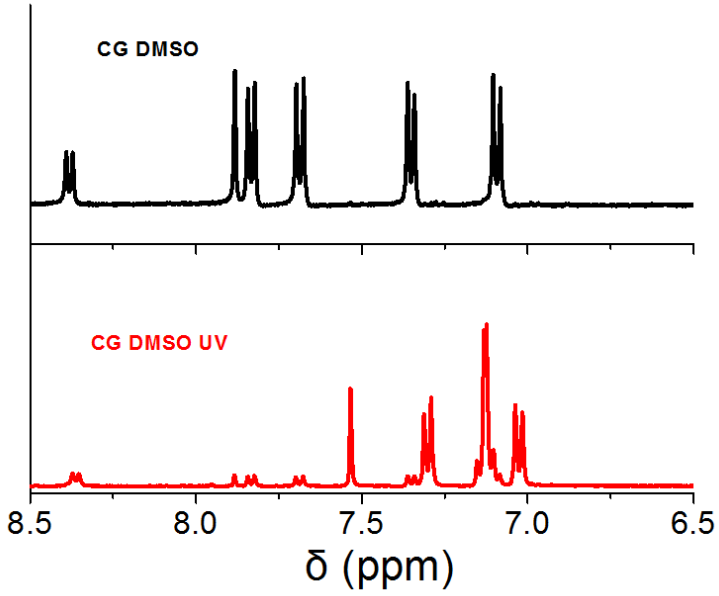

Figure S18. Stacked ^{1}H NMR spectra of CG in D_6-DMSO before and after UV irradiation for 2 hours (400 MHz, 298 K).

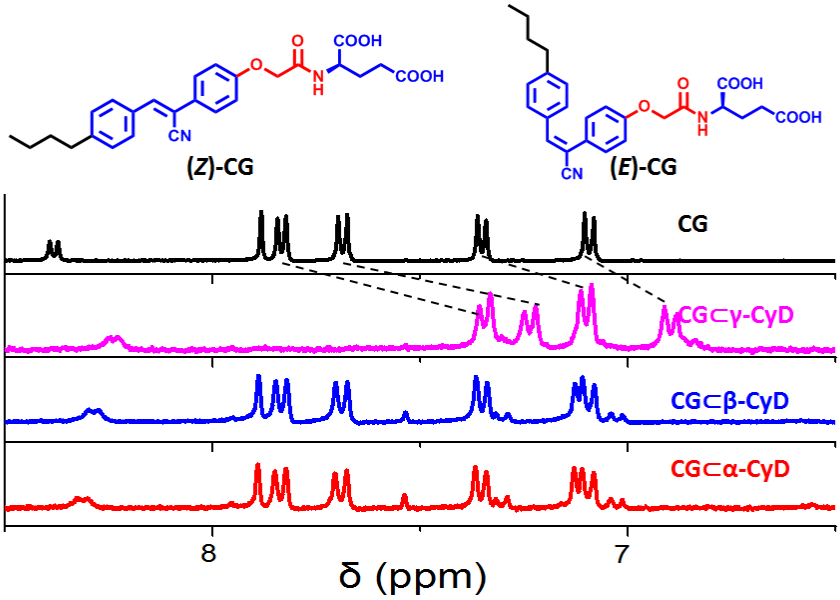

Figure S19. Stacked ^{1}H NMR spectra of CG solution and CG⊂CyD hydrogels after 2 h UV irradiation (400 MHz, D_6-DMSO, 298 K).

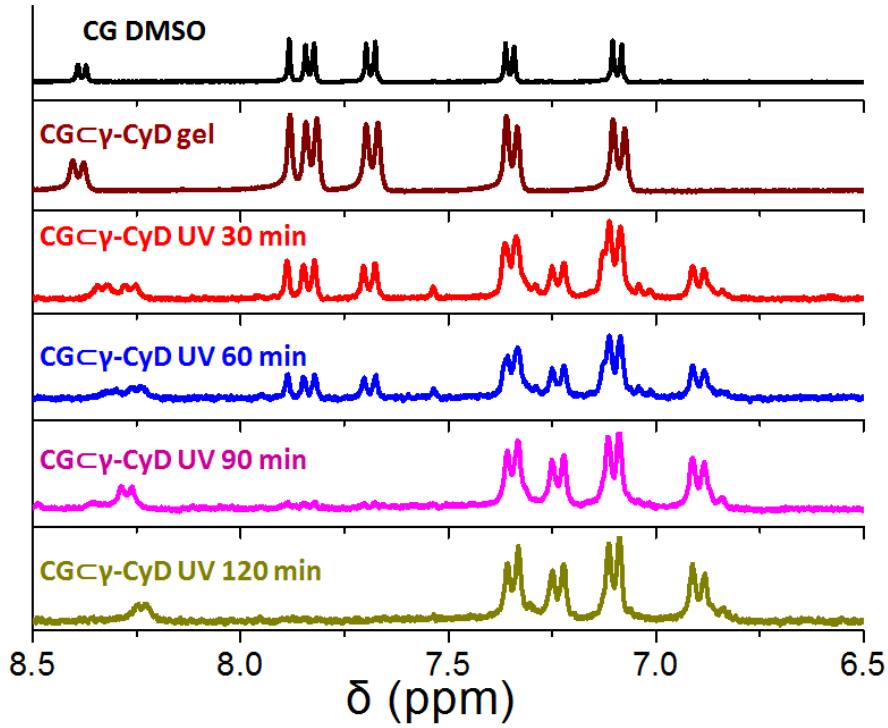

Figure S20. Stacked ^{1}H NMR spectra of the CG, CG⊂γ-CyD hydrogel before UV and CG⊂γ-CyD supra-hydrogel under different UV irradiation times. The samples were vacuum dried and dissolve in D_6-DMSO to conduct NMR tests. 400 MHz, 298 K, [CG] = [CyD] = 6.5 mM.

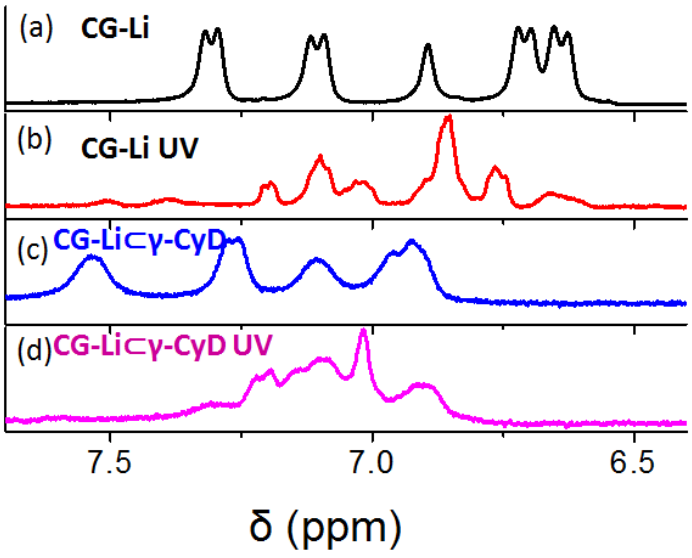

Figure S21. Stacked ^{1}H NMR spectra for (a) CG-Li and (b) CG-Li after UV, (c) CG-Li⊂γ-CyD and (d) CG-Li⊂γ-CyD after UV (400 MHz, 298 K, D_2O). The protons on aromatic showed obvious downfield for CG-Li⊂γ-CyD solution before and after UV irradiation, indicating that both (*Z*)-form and (*E*)-form CG molecule are incorporated into the cavity of γ-CyD. [CG] = [γ-CyD] = 6.5 mM. CG-Li means CG molecule exists in the form of lithium salt aqueous solution.

6. Supplementary XRD, FT-IR, DLS and rheological data.

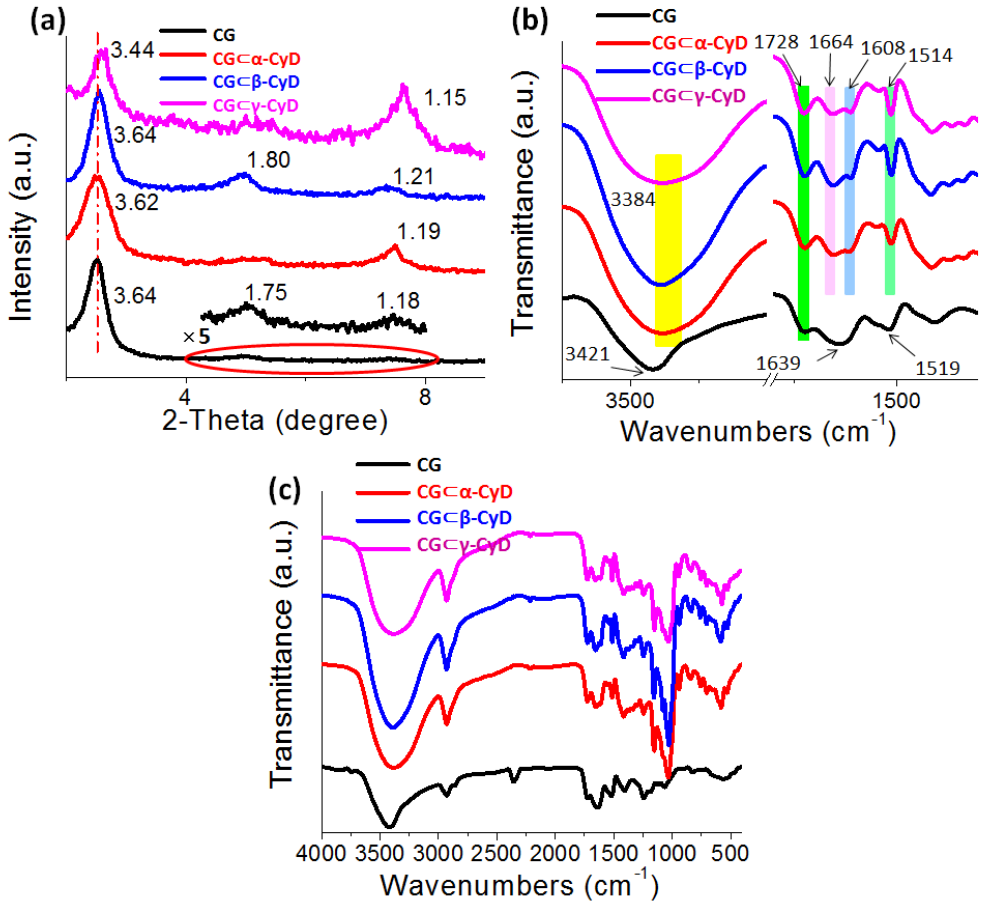

Figure S22. (a) XRD patterns for the xerogels of CG and CG⊂CyDs. (b) part of FT-IR spectra for the xerogels of CG and CG⊂CyDs, (c) full range of FT-IR spectra for the xerogels of CG and CG⊂CyDs.

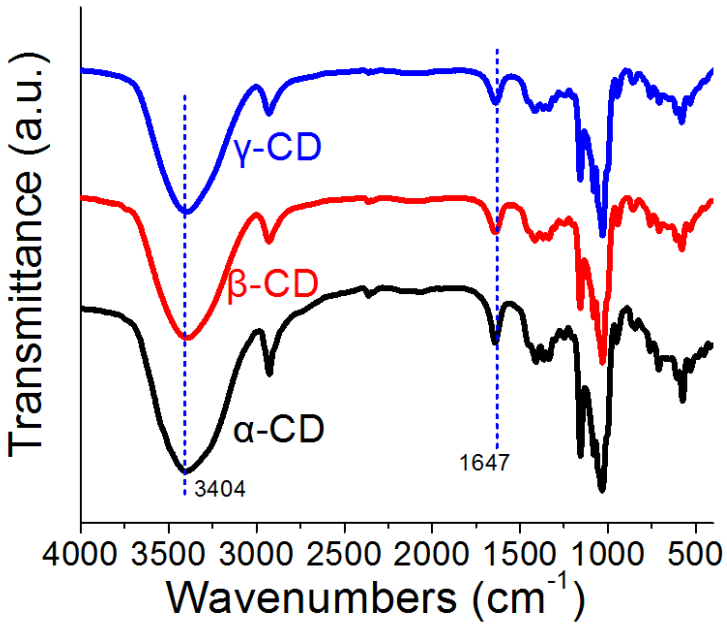

Figure S23. FT-IR spectra for the powder of pure α-, β-, and γ-CyDs.

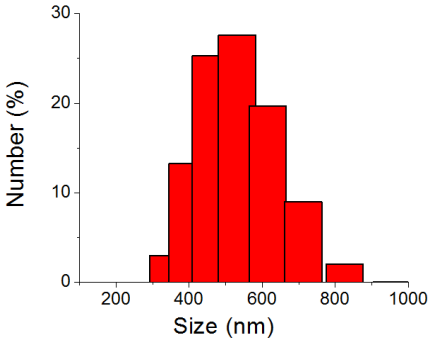

Figure S24. DLS data of CG⊂γ-CyD hydrogel after UV irradiation for two hours, the average size of the nanospheres was about 531 nm.

7. Experimental Section

Self-Assembly Procedure. A typical procedure for the hydrogel formation was as follows: 3 mg CG and equal mole amount of cyclodextrin were dispersed into 1 mL Milli-Q water and heated to form a transparent solution then naturally cooled to 25 ℃. After 10 minutes, a white supra-hydrogel was obtained. Certain amount of hydrogel was taken using a small spoon from the sample tube to conduct spectrum tests.

Characterization.

SEM & TEM: SEM images were recorded on a Hitachi S-4800 FE-SEM instrument with an accelerating voltage of 10 kV. Samples were cast onto single-crystal silica plates, the solvent was evaporated under the ambient conditions. The sample surface was coated with a thin layer of Pt to increase the contrast. TEM images were obtained on a JEM-1011 electron microscope at an accelerating voltage of 100 kV. The TEM samples were prepared by casting a small amount of sample on carbon-coated copper grids (300 meshes) and dried under strong vacuum.

XRD: XRD analysis was performed on a Rigaku D/Max-2500 X-ray diffractometer (Japan) with Cu K_α radiation (λ=1.5406 Å), which was operated at a voltage of 40 kV and a current of 200 mA. Samples were cast on glass substrates and vacuum-dried for XRD measurements.

FT-IR: FT-IR spectra were recorded on a Bruker Tensor 27 FT-IR spectrometer at room temperature. The KBr pellets made from the vacuum-dried samples of xerogels were used for FT-IR spectra measurements.

UV/Vis, CD & CPL: UV−Vis spectra were recorded in quartz plates (light path 0.1 mm) on a JASCO UV-550 spectrometer. All the samples were prepared by directly taking hydrogel from the test tube. Circular Dichroism (CD) spectra were recorded in quartz curettes (light path 0.1 mm) on a JASCO J-810 spectrophotometer. The samples were taken from the sample tube and cast on quartz plates. CPL measurements were performed with a JASCO CPL-200 spectrometer (light path 0.1 mm). The samples were prepared by directly taking hydrogel from the test tube. In

order to keep the detector at the best state and obtain the precise signals, the DV values were monitored to about 0.5 Voltage.

Fluorescence Spectra: Fluorescence spectra were recorded in quartz cuvettes (light path 1 mm) on a Hitachi F-4500 fluorescence spectrophotometer. For all the hydrogels, the EX slit and EM slit were set as 5 nm, and the PMT voltage was set as 400 V.

^{1}H NMR spectra: ^{1}H NMR spectra were recorded on a Bruker Avance 400 spectrometer, TMS as internal standard, 298 K, and the sample was dissolved in D_6-Dimethyl Sulfoxide or D_2O.

Fluorescent microscopy: It was recorded on the Olympus FV1000- IX81 confocal microscope system with 100X oil immersion objective, by using high-pressure mercury lamp as excitation source for fluorescent images.

Isothermal Titration Calorimetry. The calorimetric measurements were conducted on a TAM III microcalorimetric system with a stainless steel sample cell of 1 mL at 25.00 ± 0.01 ℃. CG-Li aqueous solution (10.0 mM) was injected into CyDs aqueous solution (2.0 mM) via a 500 μL Hamilton syringe controlled by a 612 Thermometric Lund pump until the interaction progress was completed. The CG-Li solution in the sample cell was stirred at 90 rpm with a gold propeller.